Extrapolation methods for obtaining low-lying eigenvalues of a large-dimensional shell model Hamiltonian matrix

N. Yoshinaga[1,*] and A. Arima[2]

[1]*Department of Physics, Saitama University, Saitama City 338-8570, Japan*
[2]*Science Museum, Japan Science Foundation, 2-1 Kitanomaru-koen, Chiyoda ku, Tokyo 102-0091, Japan*

We propose some new, efficient, and practical extrapolation methods to obtain a few low-lying eigenenergies of a large-dimensional Hamiltonian matrix in the nuclear shell model. We obtain those energies at the desired accuracy by extrapolation after diagonalizing small-dimensional submatrices of the sorted Hamiltonian matrix.

I. INTRODUCTION

Extrapolation provides us with an intriguing and useful method for quantum many-body problems in many fields of physics. The Hilbert spaces of quantum many-body systems can be finite, but are essentially large or infinite. In handling such large Hilbert spaces by numerical methods, we encounter various difficulties. However, if we can manage a dominant but small subspace, the contribution of the remaining huge subspace can be estimated and incorporated by some kind of extrapolation method. More concretely, we can estimate the exact energy of either the ground state or an excited state by extrapolation if we know a scaling property, such as how its energy changes as a function of a certain physical quantity.

The shell model is part of the fundamental framework of nuclear structure physics. For shell model calculations, we need to handle very huge Hilbert spaces on various occasions. One of the conventional approaches is diagonalization with spherical single-particle basis states, which recently has become applicable in the M scheme to quite large-scale problems with dimension up to 10^{10} [1,2]. However, for even larger spaces, diagonalization is impossible because of computational difficulties. To overcome this limitation of diagonalization, various methods have been developed [3–6]. Among the basis-truncation approaches, schemes based on many-body perturbation theory, such as the importance-truncation method, have been proposed [7,8].

Recently, Shen *et al.* showed that eigenvalues have a strong linear relation with diagonal matrix elements for individual runs of the two-body random ensemble or Gaussian orthogonal random matrices, if both eigenvalues and diagonal matrix elements are sorted from smaller values to larger ones [9]. They demonstrated these correlations for various cases from realistic shell model interactions to various random matrices [10,11]. Using this linear relation, we can estimate eigenenergies without diagonalization of the shell model Hamiltonian matrix.

In this paper, we propose some new, efficient, and practical extrapolation methods to obtain a few low-lying eigenenergies of a large-dimensional matrix appearing in the nuclear shell model. We obtain those energies to the desired accuracy by extrapolation after diagonalizing small-dimensional submatrices of the sorted Hamiltonian matrix.

This paper is organized as follows. In Sec. II, we exemplify some properties of the shell model Hamiltonian without and with the sorting of diagonal elements. In Sec. III, we define the submatrix after sorting the diagonal elements of the original matrix, and investigate the eigenenergies as a function of the submatrix dimension. In Sec. IV, various extrapolation methods for energies are proposed and examined. In Sec. V, we apply the extrapolation methods to estimate low-lying eigenenergies in ^{28}Si. In Sec. VI, conclusions and a summary are given.

All results in this paper are based on the shell model code of Takada [12]. Throughout this paper, all states are classified with definite spin I and positive parity, and the J scheme is used for the universal sd-shell (USD) interaction [13].

II. SORTING DIAGONAL ELEMENTS

Let us consider a shell model Hamiltonian matrix H (real and symmetric) with dimension d, whose matrix elements are denoted as $h_{ij}(i, j = 1, \ldots, d)$. The method of estimating eigenenergies $E_i(i = 1, \ldots, d)$ by the linear relation

$$E_i = ah_{ii} + b \tag{1}$$

has been found to be extremely good for most of the energies after the diagonal elements h_{ii} are sorted in increasing order [9–11]. Here a and b are related to the matrix elements,

$$a = \sqrt{\frac{\overline{H^2} - \bar{h}^2}{\overline{h^2} - \bar{h}^2}} \tag{2}$$

and

$$b = \bar{h}(1 - a), \tag{3}$$

where $\bar{h} = \text{Tr}(H)/d$, $\overline{h^2} = \sum_{i=1}^{d}(h_{ii})^2/d$, and $\overline{H^2} = \text{Tr}(H^2)/d$. Here $\text{Tr}(A)$ means the trace of a matrix A. The relation (1) is a natural consequence provided that both the diagonal elements and eigenenergies follow Gaussian distributions. Using this linear relation, we can estimate eigenenergies without diagonalization of the shell model Hamiltonian matrix. Unfortunately, it is found that the relation is not applicable for the low- or high-lying energies, although the estimation of eigenenergies is very good in the intermediate-energy regime. In this paper, we tackle
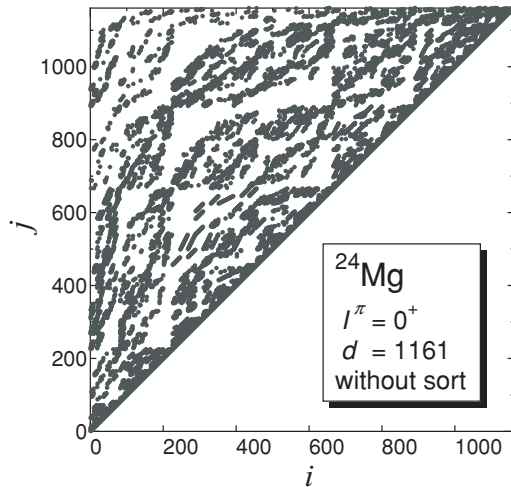
---

*yoshinaga@phy.saitama-u.ac.jp

FIG. 1. Distribution of nonzero matrix elements h_{ij} ($1 \leqslant i, j \leqslant n$) without sorting of the diagonal elements in ^{24}Mg. Those elements for $|h_{ij}| > 1.0$ are shown as dots. Since the matrix is symmetric, only the upper left components are shown.

the problem of overcoming this difficulty and obtain a few low-lying energies.

In Fig. 1, we show the distribution of matrix elements h_{ij} as the absolute value $|h_{ij}| > 1.0$ for $I^{\pi} = 0^{+}$ states in ^{24}Mg ($d = 1161$) using the USD interaction [13]. It is evident from the figure that the distribution is not smooth and is rather irregular. Next we sort the matrix elements h_{ij} such that the diagonal elements are placed from smaller values to larger ones $h_{ii}(h_{11} \leqslant h_{22} \leqslant \cdots \leqslant h_{dd})$ by changing the order of the basis states. Note that the eigenenergies $E_i (i = 1, \ldots, d)$ of the original matrix are not changed by this operation. In Fig. 2, we show the distribution of the sorted Hamiltonian matrix elements for $I^{\pi} = 0^{+}$ states in ^{24}Mg. It is seen that the distribution has now become smooth. We expect that we can incorporate the effect of off-diagonal elements on the eigenenergies smoothly when we consider the submatrices of
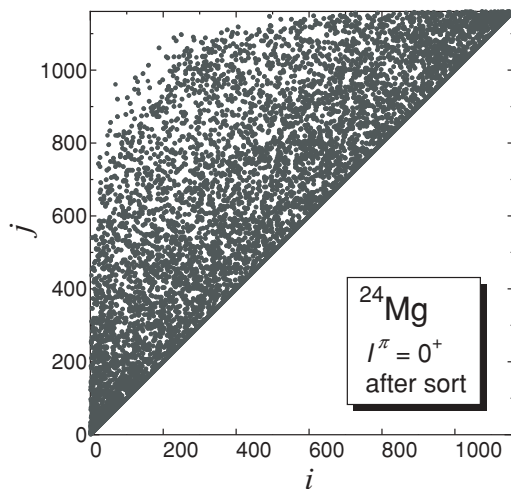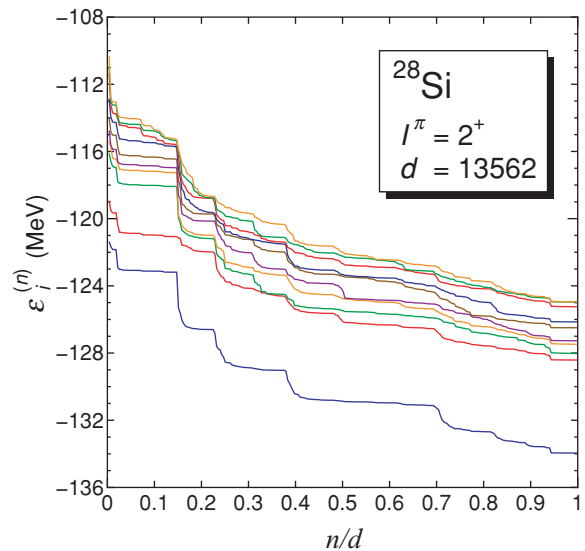

FIG. 3. (Color online) Lowest ten eigenenergies $\varepsilon_i^{(n)}$ ($i = 1, \ldots, 10$) of the submatrix with dimension n, without sorting of diagonal elements, for $I^{\pi} = 2^{+}$ states in ^{28}Si, as functions of n/d.

the original Hamiltonian after sorting its diagonal elements in increasing order.

III. PROPERTIES OF SUBMATRIX EIGENENERGIES

Let us consider a submatrix $H^{(n)}$ with dimension n whose matrix elements $h_{ij}^{(n)}$ are defined by $h_{ij}^{(n)} = h_{ij}$ ($i, j = 1, \ldots, n$) of a real symmetric matrix H with dimension d ($n \leqslant d$). After diagonalization of the submatrix $H^{(n)}$, the corresponding eigenenergies $\varepsilon_1^{(n)}, \varepsilon_2^{(n)}, \ldots, \varepsilon_n^{(n)}$ with $\varepsilon_1^{(n)} \leqslant \varepsilon_2^{(n)} \leqslant \cdots \leqslant \varepsilon_n^{(n)}$ can be understood as approximately representing exact energies $E_1, E_2, \ldots, E_n$ with $E_1 \leqslant E_2 \cdots \leqslant E_n$ for the original matrix H. In Fig. 3 we show the lowest ten eigenenergies

FIG. 2. As Fig. 1, but the elements for $|h_{ij}| > 1.0$ are shown as dots after sorting of the diagonal elements.
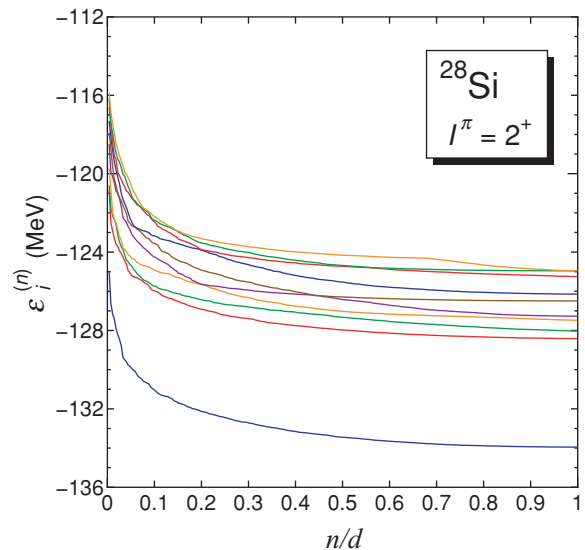

FIG. 4. (Color online) As Fig. 3, for the lowest ten eigenenergies of the submatrix with dimension n after sorting diagonal elements for $I^{\pi} = 2^{+}$ states in ^{28}Si.
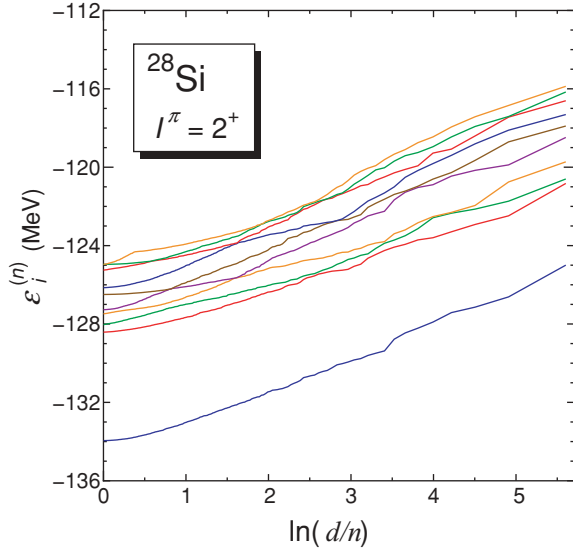
FIG. 5. (Color online) Lowest ten eigenenergies as functions of $\ln(d/n)$ for $I^\pi = 2^+$ states in ^{28}Si.
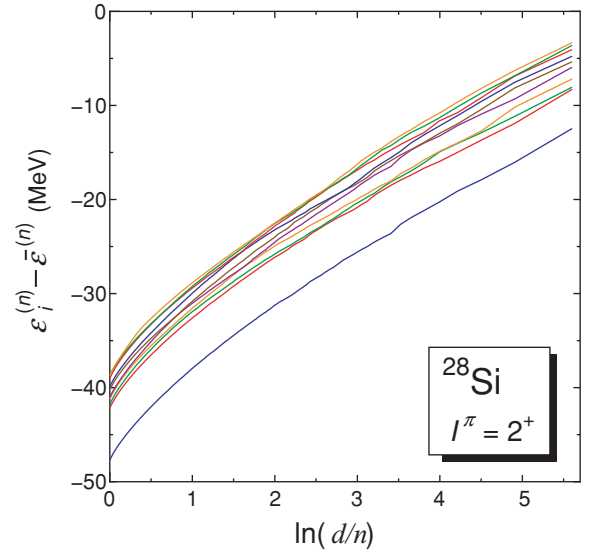

FIG. 6. (Color online) As Fig. 5, but showing $\varepsilon_i^{(n)} - \bar{\varepsilon}^{(n)}$ as functions of $\ln(d/n)$ for the lowest ten eigenenergies in ^{28}Si.

$\varepsilon_1^{(n)}, \varepsilon_2^{(n)}, \ldots, \varepsilon_{10}^{(n)}$ for $I^\pi = 2^+$ states in ^{28}Si as functions of n/d ($d = 13562$). It is seen that the eigenenergies monotonically decrease to exact eigenenergies as n/d approaches 1. However, each energy curve unexpectedly drops at certain values of n as n increases. This is because the diagonal elements h_{ii} do not change monotonically as a function of n.

Next we sort the original Hamiltonian with dimension d such that the diagonal elements are placed from smaller values to larger ones by changing the order of the basis states. In Fig. 4 we show the lowest ten eigenenergies $\varepsilon_1^{(n)}, \varepsilon_2^{(n)}, \ldots, \varepsilon_{10}^{(n)}$ for $I^\pi = 2^+$ states in ^{28}Si as functions of n/d. Now each eigenenergy decreases smoothly as n/d approaches 1.

IV. EXTRAPOLATION METHODS

As suggested in the previous section, we should sort the diagonal elements of the matrix when we consider its submatrices and evaluate the energies for the original matrix by using extrapolation methods. From now on we assume that the matrix elements are sorted such that the diagonal elements are placed from smaller values to larger ones by changing the order of the basis states. In Fig. 5 we plot the lowest ten eigenenergies of $I^\pi = 2^+$ states in ^{28}Si as functions of $\ln(d/n)$ where $\ln(d/n)$ approaches zero as n goes

to d. Here we observe the following facts: (i) Each curve is found to be approximately linear but is slightly concave up. (ii) Except for the region with large $\ln(d/n)$ (>3.0), most eigenenergies decrease smoothly as $\ln(d/n)$ approaches zero ($n = d$). However, we observe the staggering of energy for the lowest-state when $\ln(d/n)$ is large enough (>3.0). (iii) When any two curves cross, they connect smoothly to each other after the crossing, the upper curve connecting to the lower one and vice versa; the effect of avoided crossings is small.

We can make use of this linear property of each curve to predict the true eigenenergy. By choosing some range of n with $\alpha < n/d < \beta$, where α and β are some numbers, and extrapolating the energies using a linear curve, we can estimate the true eigenenergy E_i for each state i. That is, we can express the curve by putting

$$\varepsilon_i^{(n)} = a_i \ln(d/n) + b_i, \qquad (4)$$

where a_i and b_i are obtained numerically by linear approximation of the curve in the specified range ($\alpha < n/d < \beta$). By taking the limit $n \to d$, we have the predicted eigenenergy $E_i^p \equiv \varepsilon_i^{(d)} = b_i$. In Table I the results in three ranges of submatrix dimension n, $\frac{1}{20} \leqslant \frac{n}{d} \leqslant \frac{1}{10}$ (range I), $\frac{1}{10} \leqslant \frac{n}{d} \leqslant \frac{1}{5}$ (range II), and $\frac{1}{5} \leqslant \frac{n}{d} \leqslant \frac{1}{3}$ (range III), are shown in addition to

TABLE I. Exact eigenenergies and extrapolated energies (in MeV) for the lowest three $I^\pi = 2^+$ states ($i = 1, 2, 3$) in ^{28}Si obtained by extrapolation (EM-A) using $\varepsilon_i^{(n)}$ in three ranges $1/20 \leqslant n/d \leqslant 1/10$ (range I), $1/10 \leqslant n/d \leqslant 1/5$ (range II), and $1/5 \leqslant n/d \leqslant 1/3$ (range III). Here the E_i's are exact energies and the ΔE_i's indicate the difference between the exact and the predicted energy E_i^p.

i	E_i	Range I		Range II		Range III	
		E_i^p	ΔE_i	E_i^p	ΔE_i	E_i^p	ΔE_i
1	-133.950	-134.750	-0.800	-134.610	-0.660	-134.510	-0.560
2	-128.415	-128.620	-0.205	-129.120	-0.705	-128.890	-0.475
3	-128.032	-129.280	-1.248	-128.000	0.032	-127.880	-0.252

TABLE II. As Table I, but values obtained by extrapolation EM-B using $\varepsilon_i^{(n)} - \bar{\varepsilon}^{(n)}$.

i	E_i	Range I		Range II		Range III	
		E_i^p	ΔE_i	E_i^p	ΔE_i	E_i^p	ΔE_i
1	-133.950	-128.761	5.189	-129.601	4.349	-131.000	2.950
2	-128.415	-122.632	5.783	-124.113	4.302	-125.377	3.038
3	-128.032	-123.289	4.742	-122.993	5.038	-124.372	3.659

the deviation between the predicted value and the exact one, $\Delta E_i = E_i^p - E_i$, for the three lowest $I^\pi = 2^+$ states in ^{28}Si. It is seen that in all cases but one the ΔE_i's are negative, because the curves are generally concave up. We call this extrapolation method EM-A.

Each $\varepsilon_i^{(n)}$ has a crossing as a function of $\ln(d/n)$ in a relatively small range of n. To absorb the crossing, instead of just considering $\varepsilon_i^{(n)}$, we subtract $\bar{\varepsilon}^{(n)}$ from $\varepsilon_i^{(n)}$ and calculate $\varepsilon_i^{(n)} - \bar{\varepsilon}^{(n)}$, where $\bar{\varepsilon}^{(n)} = \text{Tr}[H^{(n)}]/n$. In Fig. 6 we show $\varepsilon_i^{(n)} - \bar{\varepsilon}^{(n)}$ as a function of $\ln(d/n)$ for the lowest ten $I^\pi = 2^+$ states in ^{28}Si. It is seen from the figure that now the crossings almost disappear. As for $\varepsilon_i^{(n)}$, we linearly extrapolate the energy in a certain range by putting

$$\varepsilon_i^{(n)} - \bar{\varepsilon}^{(n)} = a_i \ln(d/n) + b_i. \quad (5)$$

By taking the limit $n \to d$, we have the predicted energy $E_i^p = \varepsilon_i^{(d)} = b_i + \bar{E}$, where $\bar{E} = \text{Tr}(H)/d$. The main advantage of this method is that the extrapolation gives the upper-bound energy of each level, since each curve is concave down. In Table II the predicted energies for three ranges (ranges I–III) are shown in addition to the deviation between the predicted values and the exact ones, ΔE_i, for the three lowest levels. It is seen that in all cases ΔE_i is positive, indicating that each curve is concave down. We call this extrapolation method EM-B.

Next, we consider $[\varepsilon_i^{(n)} - \bar{\varepsilon}^{(n)}]^2/\sigma^{(n)}$, where $\sigma^{(n)}$ (>0) is the width of the submatrix defined by

$$[\sigma^{(n)}]^2 = \frac{1}{n}\text{Tr}\{[H^{(n)} - \bar{\varepsilon}^{(n)}]^2\}. \quad (6)$$

In Fig. 7 we show $[\varepsilon_i^{(n)} - \bar{\varepsilon}^{(n)}]^2/\sigma^{(n)}$ as a function of $\ln(d/n)$ for the lowest ten $I^\pi = 2^+$ states in ^{28}Si. It is also seen from the figure that this curve is almost linear except around $n/d \sim 1$. The advantage of this method is that the extrapolation gives the upper bounds for each state in most cases, since each curve is concave down around $n/d \sim 1$. Similarly, by drawing a linear

curve in a certain range of $\alpha < n/d < \beta$, we can put

$$\frac{[\varepsilon_i^{(n)} - \bar{\varepsilon}^{(n)}]^2}{\sigma^{(n)}} = a_i \ln(d/n) + b_i. \quad (7)$$

By taking the limit $n \to d$, we obtain the expression

$$E_i^p = \varepsilon_i^{(d)} = \bar{E} - \sqrt{\sigma b_i}, \quad (8)$$

where $\sigma^2 = \text{Tr}(H^2 - \bar{E}^2)/d$.

In Table III the predicted energies for three ranges (ranges I–III) are shown, in addition to the deviation between the predicted value E_i^p and the exact one, $\Delta E_i = E_i^p - E_i$, for the three lowest levels. It is seen that in most cases ΔE_i is positive. We call this extrapolation method EM-C.

V. ESTIMATION OF EIGENENERGIES

In this section we apply the extrapolation methods to obtain approximately some low-lying energies in ^{28}Si. In Fig. 8, linearly extrapolated energies are given using the data points in range I obtained by the methods EM-A, EM-B, and EM-C. In EM-A and EM-C, energies are overbound, but in EM-B the energies are upper bounds. The binding energy of the ground state is best reproduced in EM-A. In all except two cases, the ordering of energy levels is correct. The ordering of the 3^+ and 4^+ states and that of the excited 0^+ and the first 4^+ states are inverted in each extrapolation method. In Fig. 9, linearly extrapolated energies in range III are shown using the data points obtained by the three extrapolation methods. As in range I, in EM-A and EM-C, energies are overbound, but in EM-B the energies are upper bounds. The precision of the predicted energies becomes more accurate than in range I. In all cases, the ordering of energy levels is correctly reproduced, except that the excited 0^+ state lies below the first 4^+ state. Moreover, in all three cases the rotational feature seen in the exact diagonalization is well reproduced.

Finally, we evaluate the second-order correlation of the energy after obtaining the low-lying energies of the submatrix at a certain dimension n. The predicted energy for the state i

TABLE III. As Table I, but values obtained by extrapolation EM-C using $[\varepsilon_i^{(n)} - \bar{\varepsilon}^{(n)}]^2/\sigma^{(n)}$.

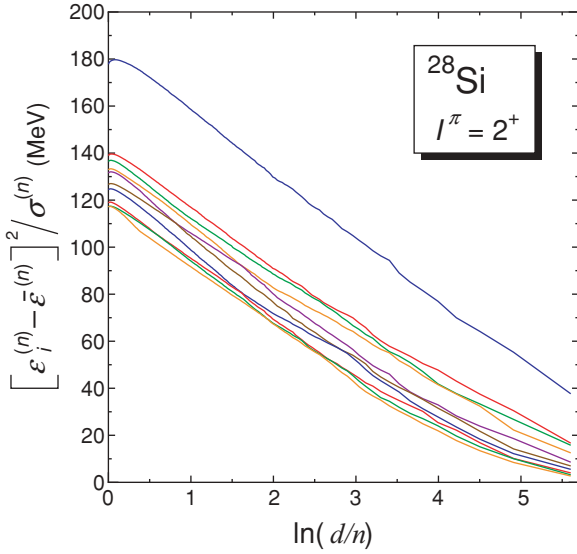| i	E_i	Range I		Range II		Range III	
		E_i^p	ΔE_i	E_i^p	ΔE_i	E_i^p	ΔE_i
1	-133.950	-134.700	-0.749	-134.870	-0.920	-135.221	-1.271
2	-128.415	-127.604	0.812	-128.645	-0.229	-129.053	-0.638
3	-128.032	-128.226	-0.194	-127.425	0.606	-127.961	0.070

FIG. 7. (Color online) As Fig. 5, but showing $[\varepsilon_i^{(n)} - \bar{\varepsilon}^{(n)}]^2/\sigma^{(n)}$ as a function of $\ln(d/n)$ in ^{28}Si.

is now given by

$$E_i^{(p)} = \varepsilon_i^{(n)} + \Delta\varepsilon_i^{\text{2nd}}, \qquad (9)$$

where the second-order perturbed energy $\Delta\varepsilon_i^{\text{2nd}}$ is calculated after diagonalizing the submatrix $H^{(n)}$. That is, we have

$$\Delta\varepsilon_i^{\text{2nd}} = -\sum_{k>n}^{d} \frac{\left[\sum_{j=1}^{n} v_j^{(i)} h_{jk}\right]^2}{h_{kk} - \varepsilon_i^{(n)}}. \qquad (10)$$

Here the coefficient $v_j^{(i)}$ is the jth component of the ith normalized eigenvector of the submatrix $H^{(n)}$, satisfying

$$\sum_{k=1}^{n} h_{jk} v_k^{(i)} = \varepsilon_i^{(n)} v_j^{(i)} \qquad (11)$$

for $1 \leqslant j \leqslant n$. Only the eigenvector for the ith state needs to be obtained. The predicted energies always give upper bounds of the true energies. In Figs. 8 and 9, the predicted energies $E_i^{(p)}$ evaluated at $n = d/10$ and $n = d/3$, respectively, are shown in
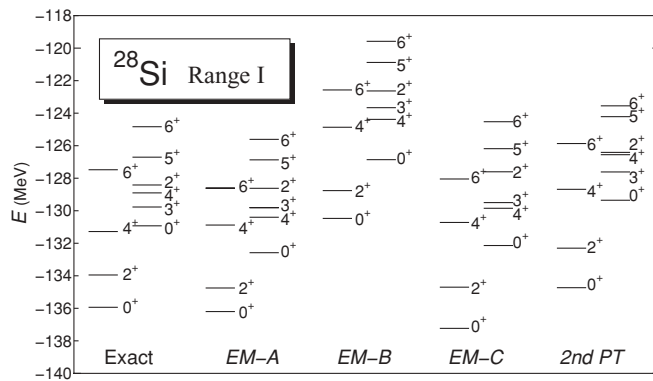

FIG. 8. Low-lying energy spectra in range I obtained by the three extrapolation methods EM-A, EM-B, and EM-C in ^{28}Si. The exact spectra and the spectra given by second-order perturbation theory (2nd PT) are shown in the first and the last column, respectively.
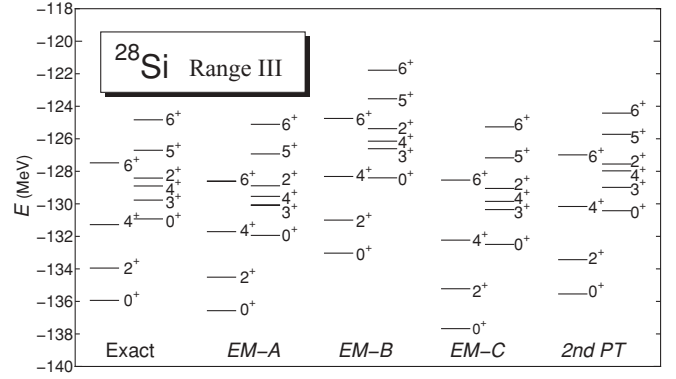

FIG. 9. As Fig. 8, but showing low-lying energy spectra in range III.

the last column. It is seen that in both cases the second-order perturbation gives better results than the other extrapolation results. In particular, in the case of $n = d/10$, the ordering of the 3^+ and 4^+ states is recovered.

VI. CONCLUSIONS

In this paper, we showed the eigenenergies of a submatrix as functions of the submatrix dimension n for a sorted large-dimensional Hamiltonian appearing in the realistic nuclear shell model. It was found to be important that the original matrix elements should be sorted so that the diagonal matrix elements are placed in increasing order. Utilizing the linear property of each energy curve, we proposed various efficient and innovative extrapolation methods to obtain a few low-lying eigenenergies. We obtained those energies to the desired accuracy by extrapolation of the energies after diagonalizing small-dimensional submatrices of the original sorted Hamiltonian matrix. Each extrapolation method gives either an upper or a lower bound for the true eigenenergy of each state for a certain large value of n. Thus, by combining these methods, we can confine the true eigenenergy within a certain range.

Throughout this paper we have used the J scheme. It would be interesting to check whether the extrapolation ranges (the n/d ratios) used in the sd-shell calculations would change or not for large-scale M-scheme calculations. We expect that our method will work better for a larger value of n; namely, the n/d ratio would be expected to be smaller for a larger value of n. However, this must be proven in future work by performing a larger-scale shell model calculation in a much larger shell such as the fp shell.

Most many-body problems in many physical fields reduce to eigenvalue problems for given Hamiltonian matrices. It is expected that the present extrapolation methods will provide us with a quite useful tool for studying such many-body problems.

[1] V. Velazquez and A. P. Zuker, Phys. Rev. Lett. **88**, 072502 (2002).

[2] J. P. Vary, P. Maris, E. Ng, C. Yang, and M. Sosonkina, J. Phys. Conf. Ser. **180**, 012083 (2009).

[3] F. J. Margetan, A. Klar, and J. P. Vary, Phys. Rev. C **27**, 852 (1983).

[4] M. Honma, T. Mizusaki, and T. Otsuka, Phys. Rev. Lett. **75**, 1284 (1995).

[5] K. Higashiyama, N. Yoshinaga, and K. Tanabe, Phys. Rev. C **67**, 044305 (2003).

[6] T. Mizusaki, Phys. Rev. C **70**, 044316 (2004).

[7] R. Roth and P. Navrátil, Phys. Rev. Lett. **99**, 092501 (2007).

[8] R. Roth, Phys. Rev. C **79**, 064324 (2009).

[9] J. J. Shen, Y. M. Zhao, A. Arima, and N. Yoshinaga, Phys. Rev. C **77**, 054312 (2008).

[10] J. J. Shen, A. Arima, Y. M. Zhao, and N. Yoshinaga, Phys. Rev. C **78**, 044305 (2008).

[11] N. Yoshinaga, A. Arima, J. J. Shen, and Y. M. Zhao, Phys. Rev. C **79**, 017301 (2009).

[12] K. Takada, shell model code JJSMQ, ftp://ftp.kutl.kyushu-u.ac.jp/ pub/takada/jjSMQ/.

[13] B. H. Wildenthal, Prog. Part. Nucl. Phys. **11**, 5 (1984); B. A. Brown and B. H. Wildenthal, Annu. Rev. Nucl. Part. Sci. **38**, 29 (1988).